Inorg. Chem. **2005**, *44*, 4309–4314

Syntheses, Structures, and Magnetic Properties of Mixed-Valent Diruthenium(II,III) Diphosphonates with Discrete and One-Dimensional Structures

Xiao-Yi Yi,[†] Bin Liu,[†] Reyes Jiménez-Aparicio,[‡] Francisco A. Urbanos,[‡] Song Gao,[§] Wei Xu,[||] Jie-Sheng Chen,[||] You Song,[†] and Li-Min Zheng*,[†]

State Key Laboratory of Coordination Chemistry, Coordination Chemistry Institute, Nanjing University, Nanjing 210093, P. R. China, Departamento de Química Inorgánica, Facultad de Ciencias Químicas, Universidad Complutense, Ciudad Universitaria, E28040-Madrid, Spain, State Key Laboratory of Rare Earth Materials and Applications, College of Chemistry and Molecular Engineering, Peking University, Beijing 100871, P. R. China, and State Key Laboratory of Inorganic Syntheses and Preparative Chemistry, Jilin University, Changchun 130023, P. R. China

Received November 23, 2004

Four mixed-valent ruthenium diphosphonates, namely, $Na_4[Ru_2(hedp)_2X]\cdot 16H_2O$ [X = Cl (**1**), Br (**2**)], $K_3[Ru_2(hedp)_2(H_2O)_2]\cdot 6H_2O$ (**3**), and $Na_7[Ru_2(hedp)_2Fe(CN)_6]\cdot 24H_2O$ (**4**), where hedp represents 1-hydroxyethylidenediphosphonate $[CH_3C(OH)(PO_3)_2]^{4-}$, were synthesized and structurally characterized. Compounds **1**, **2,** and **4** show linear chain structures in which the mixed-valent $[Ru_2(hedp)_2]^{3-}$ dimers are linked by X^- or $[Fe(CN)_6]^{4-}$ bridges. Compound **3** contains discrete species of $[Ru_2(hedp)_2(H_2O)_2]^{3-}$ where the axial positions of $[Ru_2(hedp)_2]^{3-}$ paddlewheel are terminated by water molecules. Magnetic studies show that significant antiferromagnetic exchanges are mediated between the $[Ru_2(hedp)_2]^{3-}$ (S = 3/2) units through halide bridges in compounds **1** and **2**.

Introduction

Mixed-valent diruthenium(II,III) tetracarboxylates with formula $[Ru_2(O_2CR)_4]^+$ have been of great interest due to their unique electronic and magnetic properties.[1,2] In these complexes, the effective magnetic moment per Ru_2^{5+} unit at room temperature are high ($\mu_{eff} \sim 3.8-4.3\ \mu_B$),[2,3] corresponding to three unpaired electrons in an electron configuration of $\sigma^2\pi^4\delta^2\pi^{*2}\delta^{*1}$.[4] By using metal−metal-bonded Ru_2 units as building blocks, a number of compounds with molecular and polymeric structures have been prepared.[2−3,5−9] Besides, the large zero-field splitting (∼70 cm^{-1}) exhibited by Ru_2^{5+} compounds provides possibilities of Ru_2^{5+}-incorporated compounds as potential molecule-based magnets such as single-chain molecular magnets.

Chain compounds based on Ru_2^{5+} units are commonly found. The bridging ligands, however, have been restricted to halide,[10] acetate,[11] phenazine,[12] pyrazine,[13] nitroxide

* E-mail: lmzheng@netra.nju.edu.cn.
[†] Nanjing University.
[‡] Universidad Complutense, Ciudad Universitaria.
[§] Peking University.
[||] Jilin University.

(1) Cotton, F. A.; Walton, R. A. *Multiple Bonds between Metal Atoms*, 2nd ed.; Oxford University Press: Oxford, 1993.
(2) (a) Aquino, M. A. S. *Coord. Chem. Rev.* **1998**, *170*, 141 and references therein. (b) Aquino, M. A. S. *Coord. Chem. Rev.* **2004**, *248*, 1025 and references therein.
(3) Cukiernik, F. D.; Luneau, D.; Marchon, J.-C.; Maldivi, P. *Inorg. Chem.* **1998**, *37*, 3698.
(4) Norman, G. J.; Renzoni, G. E.; Case, D. A. *J. Am. Chem. Soc.* **1979**, *101*, 5256.
(5) (a) Barral, M. C.; González-Prieto, R.; Jiménez-Aparicio, R.; Priego, J. L.; Torres, M. R.; Urbanos, F. A. *Eur. J. Inorg. Chem.* **2003**, 2339. (b) Jiménez-Aparicio, R.; Urbanos, F. A.; Arrieta, J. M. *Inorg. Chem.* **2001**, *40*, 613. (c) Barral, M. C.; Jiménez-Aparicio, R.; Pérez-Quintanilla, D.; Priego, J. L.; Royer, E. C.; Torres, M. R.; Urbanos, F. A. *Inorg. Chem.* **2000**, *39*, 65.
(6) (a) Miyasaka, H.; Clérac, R.; Campos-Fernández, C. S.; Dunbar, K. R. *J. Chem. Soc., Dalton Trans.* **2001**, 858. (b) Miyasaka, H.; Clérac, R.; Campos-Fernández, C. S.; Dunbar, K. D. *Inorg. Chem.* **2001**, *40*, 1663. (c) Miyasaka, H.; Campos-Fernández, C. S.; Clérac, R.; Dunbar, K. D. *Angew. Chem., Int. Ed.* **2000**, *39*, 3831.
(7) Yoshioka, D.; Mikuriya, M.; Handa, M. *Chem. Lett.* **2002**, 1044.
(8) (a) Liao, Y.; Shum, W. W.; Miller, J. S. *J. Am. Chem. Soc.* **2002**, *124*, 9336. (b) Vos, T. E.; Liao, Y.; Shum, W. W.; Her, J.-H.; Stephens, P. W.; Reiff, W. M.; Miller, J. S. *J. Am. Chem. Soc.* **2004**, *126*, 11630.
(9) Angaridis, P.; Berry, J. F.; Cotton, F. A.; Murillo, C. A.; Wang, X. P. *J. Am. Chem. Soc.* **2003**, *125*, 10327.
(10) (a) Bennet, M. J.; Caulton, K. G.; Cotton, F. A. *Inorg. Chem.* **1969**, *8*, 1. (b) Cotton, F. A.; Kim, Y.; Ren, T. *Polyhedron* **1993**, *12*, 607. (c) Barral, M. C.; Jiménez-Aparicio, R.; Pérez-Quintanilla, D.; Pinilla, E.; Priego, J. L.; Royer, E. C.; Urbanos, F. A. *Polyhedron* **1998**, *18*, 371.
(11) Cotton, F. A.; Matusz, M.; Zhong, B. *Inorg. Chem.* **1988**, *27*, 4368.

10.1021/ic048340z CCC: $30.25
Published on Web 04/29/2005

radicals,[14] 4,4′-bipyridine, or 1,4-diazabicyclooctane.[15] Antiferromagnetic interactions were observed in these compounds. For those containing both Ru_2^{5+} units and nitroxide radical bridges, ferrimagnetic behaviors were found with strong antiferromagnetic couplings ($J \sim -100$ cm^{-1}) between the S = 3/2 Ru_2^{5+} core and the S = 1/2 nitroxide.[14b]

Metal hexacyanide anions $[M(CN)_6]^{n-}$ (M = Cr, Fe, Co, V, Mn, etc.), as efficient building blocks, have been conventionally used in the fields of molecule-based magnets and supramolecular assemblies.[16] However, reports on the structures that combine the Ru_2^{5+} core with $[M(CN)_6]^{n-}$ linkers are rare. The first example is the compound $[Ru_2(O_2CCMe_3)_4]_3[Fe^{III}(CN)_6]\cdot 4H_2O$, which shows a two-dimensional layer structure.[7] Miller et al. carried out a detailed study on the magnetic properties of powder samples of $[Ru_2(O_2CMe)_4]_3[M^{III}(CN)_6]$ (M = Cr, Fe, Co).[8a] Long-range magnetic ordering was found at 33 K when M = Cr. The cubic three-dimensional structure of $[Ru_2(O_2CMe)_4]_3[Cr^{III}(CN)_6]$ was recently confirmed by Rietveld analysis of the synchrotron powder data.[8b] As far as we are aware, chain compounds that contain both Ru_2^{5+} and $[M(CN)_6]^{n-}$ linkers have never been reported.

Our efforts in synthesizing Ru_2^{5+}-incorporated chain compounds are based on a negatively charged diruthenium(II, III) unit $[Ru_2(hedp)_2]^{3-}$, where hedp represents 1-hydroxyethylidenediphosphonate $[CH_3C(OH)(PO_3)_2]^{4-}$. By utilizing diamagnetic halides or $[Fe(CN)_6]^{4-}$ anions as bridging ligands, linear chain compounds with the formula $Na_4[Ru_2(hedp)_2X]\cdot 16H_2O$ [X = Cl (**1**), Br (**2**)], and $Na_7[Ru_2(hedp)_2Fe(CN)_6]\cdot 24H_2O$ (**4**) have been assembled. In this paper, the structures and magnetic properties of these compounds as well as the dinuclear compound $K_3[Ru_2(hedp)_2(H_2O)_2]\cdot 6H_2O$ (**3**) are reported.

Experimental Section

Materials and Methods. Compound $(NH_4)_3[Ru_2(hedp)_2]\cdot 2H_2O$ was synthesized previously.[17] All the other starting materials were of reagent grade and were obtained from a commercial source without further purification. Elemental analyses were performed in a PE240C elemental analyzer. The infrared spectra were recorded on a VECTOR 22 spectrometer with pressed KBr pellets. Variable-temperature magnetic susceptibility data were obtained on polycrystalline samples (38.3 mg for **1**, 19.4 mg for **2**, 24.41 mg for **3**, 61.54 mg for **4**) from 1.8 to 300 K in a magnetic field of 2 kOe, using a Quantum Design MPMS-XL7 SQUID magnetometer. The data were corrected for the diamagnetic contributions of both the sample holder and the compound obtained from Pascal's constants.[18]

Synthesis of $Na_4[Ru_2(hedp)_2Cl]\cdot 16H_2O$, 1. A mixture of $(NH_4)_3[Ru_2(hedp)_2]\cdot 2H_2O$ (0.1382 g, 0.20 mmol) and a 25 mL aqueous solution of 1 M NaCl was heated at 80 °C for 4 h. After filtration, the resulting brown-red solution was allowed to stand at room temperature for 1 day. Brown rodlike crystals of compound **1** were collected by suction filtration, washed with water, and dried in air. Yield: 62% based on Ru. Anal. Calcd. for $C_4H_{40}O_{30}P_4ClNa_4Ru_2$: C, 4.70; H, 3.95%; Found: C: 4.79; H, 3.95%. IR (KBr, cm^{-1}): 3449 (br, s), 1655 (s), 1458 (m), 1364 (m), 1308 (m), 1151 (s), 1046 (m), 965 (s), 901 (ms), 818 (w), 583 (s), 489 (s), 421 (m). Thermal analysis shows that the weight loss in the temperature range 20−190 °C is 28.2%, in agreement with the calculated value for the release of sixteen water molecules (28.2%).

Synthesis of $Na_4[Ru_2(hedp)_2Br]\cdot 16H_2O$, 2. A mixture of $(NH_4)_3[Ru_2(hedp)_2]\cdot 2H_2O$ (0.0610 g, 0.0864 mmol) and a 10 mL aqueous solution of 1 M NaBr was heated at 80 °C under stirring for 4 h. The resulting brown-red filtrate was allowed to stand at room temperature. After three months, brown rodlike crystals were collected by suction filtration, washed with water, and dried in air. Yield: 47% based on Ru. Anal. Calcd. for $C_4H_{40}O_{30}P_4BrNa_4Ru_2$: C, 4.50; H, 3.78%; Found: C: 4.52; H, 3.88%. IR (KBr, cm^{-1}): 3447 (s), 1654 (s), 1629 (s), 1451 (m), 1397 (m), 1361 (m), 1306 (m), 1149 (s), 1045 (m), 964 (s), 900 (s), 818 (s), 778 (s), 579 (s), 486 (s). Thermal analysis shows that the weight loss in the temperature range 20−190 °C is 27.0%, close to the calculated value for the release of sixteen water molecules (26.4%).

Synthesis of $K_3[Ru_2(hedp)_2(H_2O)_2]\cdot 6H_2O$, 3. A mixture of $(NH_4)_3[Ru_2(hedp)_2]\cdot 2H_2O$ (0.0666 g, 0.094 mmol) and an aqueous solution of 1M KCl (15 mL), was stirred at 80 °C for 4 h. The filtrate was kept at room temperature for 22 d. Brown column-like crystals of **3** were collected, washed with water, and dried in air. Yield: 66% based on Ru. Anal. Calcd. for $C_4H_{24}O_{22}P_4K_3Ru_2$: C, 5.54; H, 2.79%; Found: C, 5.37; H, 2.91%. IR (KBr, cm^{-1}): 3412 (s), 3222 (br), 1655 (m), 1454 (w), 1440 (w), 1378 (w), 1361 (w), 1136 (s), 1098 (m), 972 (s), 962 (s), 932 (m), 902 (m), 812 (m), 708 (m), 591 (s), 576 (s), 486 (s), 437 (m). Thermal analysis reveals that the observed weight loss below 200 °C (15.1%) is close to the theoretical value (15.7%) for the removal of two coordinated and six lattice water molecules.

Synthesis of $Na_7[Ru_2(hedp)_2Fe(CN)_6]\cdot 24H_2O$, 4. A mixture of compound **1** (0.1124 g, 0.115 mmol), $Na_4[Fe(CN)_6]\cdot 3H_2O$ (0.0448 g, 0.125 mmol) and 5 mL H_2O was stirred at 80 °C for 4 h. The brown-red filtrate was allowed to stand at room temperature for 10 d. Brown column-like crystals of compound **4** were collected by suction filtration, washed with water, and dried in air. Yield: 30% based on Ru. Anal. Calcd. for $C_{10}H_{56}O_{38}P_4N_6FeNa_7Ru_2$: C, 8.50; H, 3.97; N, 5.95%. Found: C: 8.34; H, 4.02; N, 5.99%. IR (KBr, cm^{-1}): 3424 (s), 2062 (s), 2047 (s), 1637 (s), 1452 (m), 1407 (s), 1365 (m), 1155 (s), 970 (s), 903 (m), 813 (m), 586 (s), 495 (m). Thermal analysis shows that the weight loss in the temperature range 20−250 °C is 29.9%, close to the calculated value for the release of twenty four water molecules (30.6%).

Crystallographic Studies. Single crystals of dimensions 0.25 × 0.05 × 0.05 mm for **1,** 0.20 × 0.05 × 0.05 mm for **2**, 0.20 × 0.15 × 0.15 mm for **3**, and 0.25 × 0.10 × 0.10 mm for **4** were used for structural determinations on a Bruker SMART APEX

(12) Cotton, F. A.; Kim, Y.; Ren, T. *Inorg. Chem.* **1992**, *3*, 2723.
(13) Cukiernik, F. D.; Giroud-Godquin, A. M.; Maldivi, P.; Marchon, J. C. *Inorg. Chim. Acta* **1994**, *215*, 203.
(14) (a) Handa, M.; Sayama, Y.; Mikuriya, M.; Nukada, R.; Hiromitsu, I.; Kasuga, K. *Bull. Chem. Soc. Jpn.* **1995**, *68*, 1647. (b) Handa, M.; Sayama, Y.; Mikuriya, M.; Nukada, R.; Hiromitsu, I.; Kasuga, K. *Chem. Lett.* **1996**, *201*. (c) Sayama, Y.; Handa, M.; Mikuriya, M.; Nukada, R.; Hiromitsu, I.; Kasuga, K. *Chem. Lett.* **1998**, 777. (d) Handa, M.; Sayama, Y.; Mikuriya, M.; Nukada, R.; Hiromitsu, I.; Kasuga, K. *Bull. Chem. Soc. Jpn.* **1998**, *71*, 119.
(15) Beck, E. J.; Drysdale, K. D.; Thompson, L. K.; Li, L.; Murphy, C. A.; Aquino, M. A. S. *Inorg. Chim. Acta* **1998**, *279*, 121.
(16) For example: (a) Dunbar, K. R.; Heintz, R. A. *Prog. Inorg. Chem.* **1997**, *45*, 283. (b) Iwamoto, T. *Comprehensive Supramolecular Chemistry*; Atwood, J. L., Davies, J. E. D., MacNicol, D. D., Vögtle, F., Toda, F., Bishop, R., Eds.; Pergamon: Oxford, 1996; Vol. 6, pp 643−690. (c) Ohba, M.; Ōkawa, H. *Coord. Chem. Rev.* **2000**, *198*, 313. (d) Černák, J.; Orendáč, M.; Potočňák, I.; Chomič, J.; Orendáčová, A.; Skoršepa, J.; Feher, A. *Coord. Chem. Rev.* **2002**, *224*, 51.
(17) Yi, X.-Y.; Zheng, L.-M.; Xu, W.; Feng, S. *Inorg. Chem.* **2003**, *42*, 2827.
(18) Kahn, O. *Molecular Magnetism*; VCH Publishers: New York, 1993.

Table 1. Crystallographic Data for Compounds **1**−**4**

	1 $C_4H_{40}O_{30}P_4ClNa_4Ru_2$	**2** $C_4H_{40}O_{30}P_4BrNa_4Ru_2$	**3** $C_4H_{24}O_{22}P_4K_3Ru_2$	**4** $C_{10}H_{56}O_{38}P_4N_6\ FeNa_7Ru_2$
MW	1021.79	1066.25	867.55	1411.41
crystal system	triclinic	triclinic	monoclinic	triclinic
space group	*P*-1	*P*-1	$P2_1/n$	*P*-1
a/Å	7.5019(15)	7.6568(13)	9.4925(16)	11.4854(18)
b/Å	10.996(2)	10.952(2)	14.476(3)	11.7200(18)
c/Å	11.585(3)	11.547(2)	9.7163(16)	11.7770(18)
α/°	61.872(3)	61.811(3)		67.254(3)
β/°	88.680(4)	88.648(4)	113.348(3)	61.284(3)
γ/°	77.460(4)	77.057(4)		64.113(3)
V/Å^3	819.2(3)	827.9(3)	1225.8(4)	1219.0(3)
Z	1	1	2	1
D_c/g cm^{-3}	2.071	2.139	2.350	1.923
F(000)	513	531	858	713
GOF on F^2	0.634	0.685	1.075	0.974
R1,wR2[a] [$I > 2\sigma(I)$]	0.0561, 0.0728	0.0543, 0.0887	0.0674, 0.0842	0.0628, 0.1103
(all data)	0.1374, 0.0883	0.1258, 0.1059	0.1053, 0.0930	0.0952, 0.1207
$(\Delta\rho)_{max}$, $(\Delta\rho)_{min}$/e Å^{-3}	0.943, −0.825	0.840, −1.045	0.974, −0.993	1.513, −0.910

[a] $R_1 = \Sigma||F_o| - |F_c||/\Sigma|F_o|$, $wR_2 = [\Sigma w(F_o^2 - F_c^2)^2/\Sigma w(F_o^2)^2]^{1/2}$.

CCD diffractometer using graphite-monochromatized Mo Kα radiation ($\lambda = 0.71073$ Å) at room temperature. A hemisphere of data was collected in the θ range 2.00−27.98° for **1**, 2.01−28.02° for **2**, 2.54−28.02° for **3**, and 1.98−28.08° for **4**, using a narrow-frame method with scan widths of 0.30° in ω and an exposure time of 10 s/frame. Numbers of observed and unique [$I > 2\sigma$ (I)] reflections are 4958 and 3633 ($R_{int} = 0.0716$) for **1**, 4984 and 3659 ($R_{int} = 0.0799$) for **2**, 7402 and 2829 ($R_{int} = 0.0658$) for **3**, and 7432 and 5447 ($R_{int} = 0.0445$) for **4**, respectively. The data were integrated using the Siemens SAINT program,[19] with the intensities corrected for Lorentz factor, polarization, air absorption, and absorption due to variation in the path length through the detector faceplate. The structures were solved by direct method and refined on F^2 by full-matrix least squares using SHELXTL.[20] All the non-hydrogen atoms in the four compounds were refined anisotropically. All the hydrogen atoms, except those of hydroxy groups and water molecules, were placed in calculated positions. The hydrogen atoms of hydroxy groups and water molecules were located from the difference Fourier maps and refined isotropically with the isotropic vibration parameters related to the non-H atom to which they are bonded. Crystallographic and refinement details of compounds **1**−**4** are listed in Table 1; selected bond lengths and angles are listed in Tables 2 and 3.

Table 2. Selected Bond Lengths [Å] and Angles [°] for Compounds **1** and **2**[a]

	1	2
Ru(1)−Ru(1A)	2.3591(16)	2.3480(15)
Ru(1)−X(1)	2.5717(9)	2.6547(9)
Ru(1)−O(1)	2.020(5)	2.033(5)
Ru(1)−O(2A)	2.042(5)	2.052(5)
Ru(1)−O(4)	2.042(5)	2.056(5)
Ru(1)−O(5A)	2.042(5)	2.035(5)
O(4)−Ru(1)−O(2A)	89.9(2)	90.4(2)
O(4)−Ru(1)−O(5A)	175.4(2)	175.2(2)
O(2A)−Ru(1)−O(5A)	89.2(2)	89.0(2)
O(4)−Ru(1)−O(1)	91.1(2)	90.4(2)
O(2A)−Ru(1)−O(1)	175.7(2)	175.2(2)
O(5A)−Ru(1)−O(1)	89.5(2)	89.8(2)
O(4)−Ru(1)−Ru(1A)	92.22(15)	92.32(15)
O(2A)−Ru(1)−Ru(1A)	91.88(15)	91.81(16)
O(5A)−Ru(1)−Ru(1A)	92.28(15)	92.45(16)
O(1)−Ru(1)−Ru(1A)	92.22(14)	92.91(15)
O(4)−Ru(1)−Cl(1)	86.65(14)	86.61(15)
O(2A)−Ru(1)−Cl(1)	89.19(14)	89.42(15)
O(5A)−Ru(1)−Cl(1)	88.86(15)	88.62(16)
O(1)−Ru(1)−Cl(1)	86.73(14)	85.88(15)
Ru(1A)−Ru(1)−Cl(1)	178.45(5)	178.38(5)

[a] Symmetry transformations used to generate equivalent atoms: A, $-x+1, -y, -z$; B, $-x, -y-2, -z+1$; C, $-x, -y-1, -z+1$; D, $-x, -y, -z$.

Results and Discussion

Crystal Structures of 1 and 2. Compounds **1** and **2** are isomorphous, crystallizing in space group $P\bar{1}$. Figure 1 shows a fragment of the linear chain structure of compound **1** in which the mixed-valent units of $[Ru_2(hedp)_2]$ with a lantern-type geometry are connected by Cl^- anions. Each Ru atom has a slightly distorted octahedral environment with four equatorial positions occupied by phosphonate oxygens of hedp and one axial site by the equivalent Ru atom. The remaining axial position is filled with chloride anion. The Ru−O bond lengths [2.020(5)−2.042(5) Å] and the Ru−Ru distance [2.359(2) Å] are comparable to those in $(NH_4)_3[Ru_2(hedp)_2]\cdot 2H_2O$ [2.023(4)−2.283(4) Å, 2.354(1) Å].[17] The Ru−Cl bond distance [2.572(1) Å] is in agreement with those found in $Ru_2(O_2CR)_4X$ [2.517−2.587 Å].[2] The hedp group serves as a bis(chelating) bridging ligand to link the two ruthenium ions into a dimer of $[Ru_2(hedp)_2]^{3-}$. The chloride anion behaves as a second bridging ligand and connects the $[Ru_2(hedp)_2]^{3-}$ units into an infinite linear chain along the *a*-axis (Figure 1). Hydrogen bonds exist between the neighboring chains with the shortest contact of 2.855(12) Å for O(7)···O(7), leading to the formation of an anionic layer of $\{Ru_2(hedp)_2Cl\}_n^{4n-}$ (Figure S1).

There are two types of sodium ions in structure **1**, each of which has a distorted octahedral environment. The Na−O distances range from 2.339(6) to 2.518(8) Å. The NaO_6 octahedra are each edge-shared with its neighbors, forming a zigzag chain running along the *b*-axis with composition $\{Na_4(H_2O)_{16}\}_n$ (Figure S2). The adjacent chains are connected through hydrogen bonds, hence resulting in a two-dimensional supramolecular layer. The anionic layers of

(19) *SAINT, Program for Data Extraction and Reduction*; Siemens Analytical X-ray Instruments Inc.: Madison, WI 53719, 1994−1996.
(20) Sheldrick, G. M. *SHELXTL, Program for Refinement of Crystal Structures*; Siemens Analytical X-ray Instruments Inc.: Madison, WI 53719, 1994.

Table 3. Selected Bond Lengths [Å] and Angles [°] for Compounds **3** and **4**

Compound **3**[a]			
Ru(1)−Ru(1A)	2.3412(11)	Ru(1)−O(1)	2.026(4)
Ru(1)−O(2A)	2.021(4)	Ru(1)−O(4)	2.028(4)
Ru(1)−O(5A)	2.031(4)	Ru(1)−O(1W)	2.309(5)
O(2A)−Ru(1)−O(1)	174.58(18)	O(2A)−Ru(1)−O(4)	89.87(17)
O(1)−Ru(1)−O(4)	89.93(17)	O(2A)−Ru(1)−O(5A)	91.28(17)
O(1)−Ru(1)−O(5A)	88.43(17)	O(4)−Ru(1)−O(5A)	174.72(18)
O(2A)−Ru(1)−O(1W)	88.51(18)	O(1)−Ru(1)−O(1W)	86.08(18)
O(4)_−Ru(1)−O(1W)	86.10(17)	O(5A)−Ru(1)−O(1W)	88.79(17)
O(2A)−Ru(1)−Ru(1A)	92.24(13)	O(1)−Ru(1)−Ru(1A)	93.18(13)
O(4)−Ru(1)−Ru(1A)	92.74(12)	O(5A)−Ru(1)−Ru(1A)	92.36(13)
O(1W)−Ru(1)−Ru(1A)	178.61(13)		
Compound **4**[b]			
Ru(1)−Ru(1A)	2.3800(10)	Ru(1)−O(1)	2.037(4)
Ru(1)−O(2A)	2.034(4)	Ru(1)−O(4)	2.040(4)
Ru(1)−O(5A)	2.032(4)	Ru(1)−N(1)	2.268(5)
Fe(1)−C(3)	1.919(6)	Fe(1)−C(4)	1.894(6)
Fe(1)−C(5)	1.917(7)		
O(2A)−Ru(1)−O(1)	176.50(15)	O(2A)−Ru(1)−O(4)	90.50(16)
O(1)−Ru(1)−O(4)	88.73(16)	O(2A)−Ru(1)−O(5A)	90.17(16)
O(1)−Ru(1)−O(5A)	90.39(16)	O(4)−Ru(1)−O(5A)	176.41(15)
O(2A)−Ru(1)−N(1)	85.62(17)	O(1)−Ru(1)−N(1)	90.96(17)
O(4)−Ru(1)−N(1)	89.30(17)	O(5A)−Ru(1)−N(1)	87.24(17)
O(2A)−Ru(1)−Ru(1A)	90.16(11)	O(1)−Ru(1)−Ru(1A)	93.29(11)
O(4)−Ru(1)−Ru(1A)	92.39(10)	O(5A)−Ru(1)−Ru(1A)	91.13(11)
N(1)−Ru(1)−Ru(1A)	175.47(13)		

[a] Symmetry transformations used to generate equivalent atoms: A: $-x+2, -y+2, -z+1$. [b] Symmetry transformation used to generate equivalent atoms: A: $-x, -y+2, -z+1$.

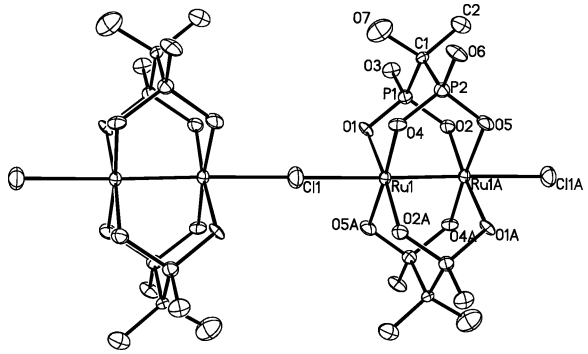

Figure 1. A fragment of the $\{Ru_2(hedp)_2Cl\}_n^{4n-}$ linear chain in structure **1** with the atomic labeling scheme (thermal ellipsoids shown at 50% probability). All H atoms are omitted for clarity.

$\{Ru_2(hedp)_2Cl\}_n^{4n-}$ and cationic layers of $\{Na_4(H_2O)_{16}\}_n^{4n+}$ are stacked alternatively with extensive hydrogen bonds between the neighboring layers, leading to a three-dimensional (3D) network structure (Figure S3).

The structure of compound **2** is analogous to that of **1** except that Cl^- is replaced by Br^-. Consequently, the cell volume increases from 819.2(3) $Å^3$ in **1** to 827.9(3) $Å^3$ in **2**. The Ru−Br bond distance [2.655(1) Å] is longer compared with the Ru−Cl bond length [2.572(1) Å]. The Ru−Ru distance is 2.348(2) Å in this case, slightly shorter than the same distance in **1**.

Crystal Structure of 3. Compound **3** crystallizes in space group $P2_1/n$. The structure consists of discrete $[Ru_2(hedp)_2(H_2O)_2]^{3-}$ dimers, potassium ions, and lattice water. The axial positions of the $[Ru_2(hedp)_2]^{3-}$ core are terminated by two water molecules (Figure 2). The Ru(1)−Ru(1A) distance is 2.341(1) Å. The Ru−O bond lengths fall in the range of 2.021(4) − 2.309(5) Å, which are comparable to those in compounds **1** and **2** although the axial Ru−O

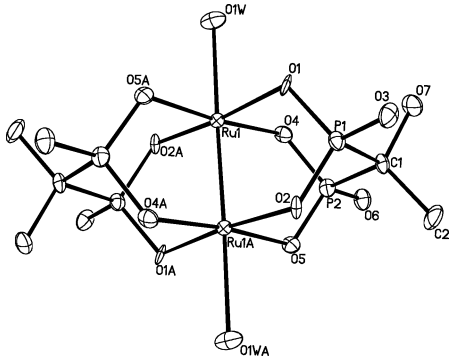

Figure 2. The $[Ru_2(hedp)_2(H_2O)_2]^{3-}$ dimer in compound **3** with the atomic labeling scheme (thermal ellipsoids shown at 50% probability). All H atoms are omitted for clarity.

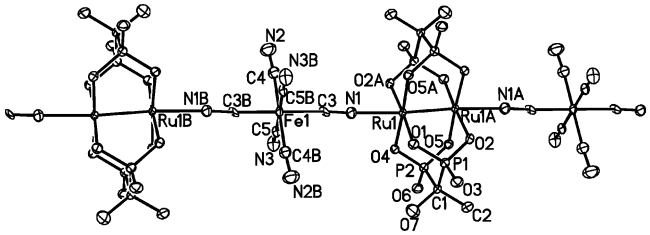

Figure 3. A fragment of the $\{Ru_2(hedp)_2Fe(CN)_6\}_n^{7n-}$ linear chain in structure **4** with the atomic labeling scheme (thermal ellipsoids shown at 50% probability). All H atoms are omitted for clarity.

distances are relatively longer. These $[Ru_2(hedp)_2(H_2O)_2]^{3-}$ dimers are cross-linked through hydrogen bonds [O(3)···O(7): 2.674(6) Å], forming anionic supramolecular layers in the *bc* plane (Figure S4). The K^+ cations and lattice water fill the intra- and interlayer spaces.

Crystal Structure of 4. Compound **4** crystallizes in space group $P\bar{1}$. It has a linear chain structure similar to those in compounds **1** and **2**, except that the halide anions in the latter are substituted by $[Fe(CN)_6]^{4-}$ anions (Figure 3). The elongation of the Ru−Ru distance in **4** [2.380(1) Å] compared with those in **1**−**3** could be caused by the axial coordination by cyanide ligand. Each Ru has a distorted octahedral geometry. The equatorial Ru−O [2.032(4)−2.040(4) Å] and the axial Ru(1)−N(1) [2.268(5) Å] bond lengths are normal. The $[Fe(CN)_6]^{4-}$ anion serves as a bridging ligand, by using two of its six cyanide anions in a trans manner, and links the $Ru_2(hedp)_2^{3-}$ units into a highly negatively charged linear chain of $\{Ru_2(hedp)_2Fe(CN)_6\}_n^{7n-}$ (Figure 3). The adjacent chains are connected by hydrogen bonds between the hydroxy group of $[Ru_2(hedp)_2]^{3-}$ and the terminal CN^- ligand of $[Fe(CN)_6]^{4-}$ [O(7)···N(2): 2.811(7) Å], forming an anionic layer (Figure S5).

Four types of sodium ions are present in structure **4** in which the Na(4) atom sits at an inversion center. All Na atoms have distorted octahedral environments except Na(2), which is five-coordinated. The Na−O distances range from 2.292(6) to 2.713(8) Å. The NaO_6 and NaO_5 polyhedra are each edge-shared or corner-shared with its neighbors, forming a zigzag chain with composition $\{Na_7(H_2O)_{24}\}_n^{7n+}$ (Figure S6). These chains penetrate through the supramolecular layer of $\{Ru_2(hedp)_2Fe(CN)_6\}_n^{7n-}$ via the coordination of Na(4) atoms with O(7) atoms from the hydroxy group of $[Ru_2(hedp)_2]^{3-}$ units [Na(4)−O(7): 2.495(4) Å].

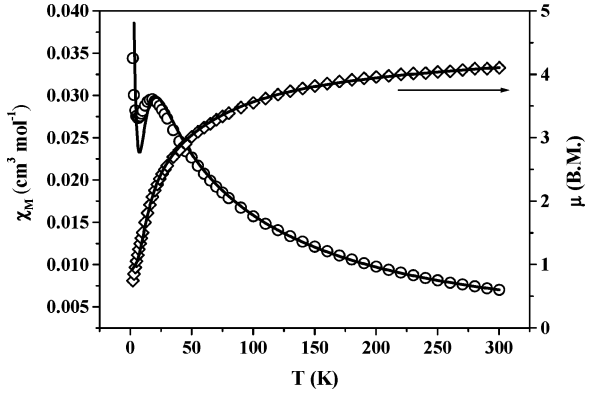

Figure 4. The χ_M and μ_{eff} vs T plots for compound **1**.

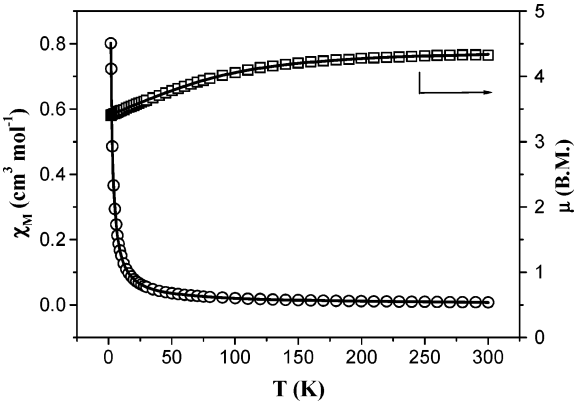

Figure 5. The χ_M and μ_{eff} vs T plots for compound **3**.

Extensive hydrogen bonds exist between the $\{Na_7(H_2O)_{24}\}_n^{7n+}$ chains. Again, a 3D supramolecular structure is built up.

Magnetic Properties. The temperature-dependent magnetic susceptibilities of compounds **1**−**4** were investigated in the temperature range 1.8 to 300 K. The observed effective magnetic moments per Ru_2 at 300 K are 4.10 μ_B for **1**, 3.76 μ_B for **2**, 4.32μ_B for **3**, and 4.37 μ_B for **4**, respectively, corresponding to three unpaired electrons. Figure 4 shows the χ_M and μ_{eff} versus T curves for compound **1**. Clearly, the χ_M value increases continuously on cooling from room temperature until approaching a maximum of 0.0295 cm^3 mol^{-1} at 18 K. Then it decreases, reaching a minimum of 0.0273 cm^3 mol^{-1} at 6 K, below which χ_M increases again. The maximum appearing in the χ_M vs T curve indicates a significant antiferromagnetic interaction between the Ru_2^{5+} dimers through the chloride bridge. The upturn of the χ_M value below 6 K could be attributed to paramagnetic impurities. Dominant antiferromagnetic exchange coupling is also observed in compound **2** between the Ru_2^{5+} dimers through the bromide bridge. The maximum appears at 22 K in the χ_M vs T curve (Figure S7).

The magnetic data of compounds **1** and **2** were fitted using a model which considers the Hamiltonian $-2JS_1S_2 + D(S_{z1}^2 + S_{z2}^2) + \mu gSH$ where D represents the zero-field splitting, J the antiferromagnetic coupling, and H the applied magnetic field. Terms corresponding to the temperature-independent paramagnetism (TIP) and a paramagnetic impurity (p) were also included in this model. The equations are quite long and will not be written here.[5b] The best fits, shown as solid lines in Figures 4 and S7, led to parameters $g = 2.1$ (fixed), $D = 78.3$ cm^{-1}, $zJ = -4.6$ cm^{-1}, TIP = 7.7×10^{-4} cm^3 mol^{-1}, $p = 6.4\%$ for **1**, and $g = 2.1$(fixed), $D = 92.1$ cm^{-1}, $zJ = -4.9$ cm^{-1}, TIP = 5.9×10^{-10} cm^3 mol^{-1}, $p = 4.4\%$ for **2**, respectively. The quality of the fits decreases when the g value increases from 2.1 to 2.2−2.3 for both complexes.

For compound **3** which is essentially a Ru_2^{5+} dimer with interdimer hydrogen bond interactions, the continuous decreasing of μ_{eff} upon cooling is mainly due to the large zero-field splitting arising from the S = 3/2 ground state of Ru_2^{5+} (Figure 5). The susceptibility data were fitted by the model of Cukiernik et al.[3] The final expression of this model is

$$\chi_M = (1 - p)\chi' + pNg_{mo}^2\beta^2/4kT$$

where p is the paramagnetic impurity, and χ' includes the antiferromagnetic coupling (zJ). Thus

$$\chi' = \chi_{M'}/[1 - (2zJ/Ng^2\beta^2)\chi_{M'}]$$

where

$$\chi_{M'} = (\chi_{||} + 2\chi_{\perp})/3 + \mathrm{TIP}$$

and

$$\chi_{||} = (Ng^2\beta^2/kT)(1 + 9e^{-2D/kT})/[4(1 + e^{-2D/kT})]$$

$$\chi_{\perp} = (Ng^2\beta^2/kT)[4 + (3kT/D)(1 - e^{-2D/kT})]/[4(1 + e^{-2D/kT})]$$

The best fit, shown as the solid line in Figure 5 , resulted in parameters $g = 2.26$, $D = 96.0$ cm^{-1}, $zJ = -0.007$ cm^{-1}, TIP = 2.4×10^{-5} cm^3 mol^{-1}, $p = 4.6 \times 10^{-5}$ %.

The magnetic behavior of compound **4** can also be treated in a similar way to compound **3** because the Ru_2^{5+} centers are linked by diamagnetic $[Fe(CN)_6]^{4-}$ anions. The best fit, shown as the solid line in Figure S8, gave parameters $g = 2.30$, $D = 101.6$ cm^{-1}, $zJ = -0.044$ cm^{-1}, TIP = 9.6×10^{-10} cm^3 mol^{-1}, $p = 2.4 \times 10^{-7}$ %.

It has been reported that the magnetic properties of the mixed-valent diruthenium compounds with formula $Ru_2(\mu\text{-}O_2CR)_4L$ can be influenced by the nature of the different axial ligands as well as the interdimer angles within the chain. For compounds $Ru_2(\mu\text{-}O_2CR)_4Cl$ in which Cl^- bridges the Ru_2^{5+} units, the existence and magnitude of interdimer antiferromagnetic exchanges could be related to the Ru−Cl−Ru angle.[3,11] When this angle is close to 180°, the strongest interaction would be found in the complex. With decreasing interdimer angle, the antiferromagnetic exchange decreases. Consequently, compounds $Ru_2(O_2CR)_4Cl$ (R = CH_2CH_3, CMeCHEt, $CMePh_2$) with a Ru−Cl−Ru angle of 180° have J values varying from −7.43 to −13.30 cm^{-1},[5b,10b] whereas the complexes forming zigzag chains or discrete molecules show weak antiferromagnetic coupling.[3,5c]

In compounds **1** and **2**, the chain structures are strictly linear with a Ru−X−Ru angle of 180°. Significant antiferromagnetic exchange would be expected through the halide bridges. Indeed, both compounds exhibit maxima in the χ_M vs T curves at ca. 18 K for **1** and 22 K for **2**. The zJ values calculated for **1** and **2** are −4.6 cm^{-1} and −4.9 cm^{-1},

respectively. Compared with $Ru_2(O_2CR)_4Cl$ ($R = CH_2CH_3$, CMeCHEt, $CMePh_2$), the antiferromagnetic couplings for **1** and **2** are weaker in accordance with the apparition of the maxima in the χ_M vs T curves at lower temperatures. However, complex **4** with a similar linear chain structure shows only very weak antiferromagnetic coupling because the diamagnetic $[Fe(CN)_6]^{4-}$ groups make difficult the magnetic interaction between the diruthenium centers.

Conclusion. This paper reports four new diruthenium(II,III) diphosphonate compounds with formula $Na_4[Ru_2(hedp)_2X]\cdot 16H_2O$ [X = Cl (**1**), Br (**2**)], $K_3[Ru_2(hedp)_2(H_2O)_2]\cdot 6H_2O$ (**3**) and $Na_7[Ru_2(hedp)_2Fe(CN)_6]\cdot 24H_2O$ (**4**) (hedp = 1-hydroxyethylidenediphosphonate). Although discrete molecular structure is found in **3**, compounds **1**, **2**, and **4** show linear chain structures where the mixed-valent $[Ru_2(hedp)_2]^{3-}$ cores are linked by X^- or $[Fe(CN)_6]^{4-}$ bridges. Dominant antiferromagnetic exchange couplings were observed for compounds **1** and **2**, while the magnetic behaviors of compounds **3** and **4** are mainly due to the large zero-field splitting of a single Ru_2^{5+} dimer. Further work is in progress to prepare chain complexes combining $[Ru_2(hedp)_2]^{3-}$ cores with paramagnetic linkers such as $[M^{III}(CN)_6]^{3-}$ (M = Fe, Cr) which could be of great interest in molecular magnetism.

Acknowledgment. We thank the NNSF of China (No. 20325103), the Ministry of Education of China, and NSF of Jiangsu province (No. BK2002078) for financial support, and Mr. Yong-Jiang Liu for crystal data collection.

Supporting Information Available: Eight figures and X-ray crystallographic files for the four compounds. This material is available free of charge via the Internet at http://pubs.acs.org.

IC048340Z